Computational Mechanics 28 (2002) 202–211 © Springer-Verlag 2002
DOI 10.1007/s00466-001-0281-z

Electrophoretic motion of two solid particles embedded in an unbounded and viscous electrolyte

A. Sellier

Abstract This work determines the electrophoretic motion of two colloidal particles embedded in a viscous and unbounded electrolyte. Contrary to other works in the field, the advocated method does not calculate the perturbation electric potential and the electrolyte Stokes flow in the whole fluid domain and its range of applications is not restricted to the case of uniformly charged particles embedded in a uniform electric field $\mathbf{E}_\infty$. The idea consists in establishing and solving thirteen Fredholm boundary integral equations (one of the second kind plus twelve of the first kind). The numerical implementation is briefly reported. Numerical benchmarks and new results are both presented and discussed with a special attention to the interactions between the particles.

Keywords Particle motion, Viscous electrolytes

1 Introduction and assumptions

We consider a colloidal solution consisting of charged and solid particles embedded in an unbounded and viscous electrolyte of constant permittivity ϵ and viscosity μ. Under the application of the external electric field $\mathbf{E}_\infty$, each charged particle moves and this phenomenon is termed electrophoresis.

In many applications to particle analysis or separation it is of the utmost interest to determine the electrophoretic motion of any solid particle $\mathcal{P}$ of smooth boundary $\mathcal{S}$ (see Fig. 1). This is usually achieved by resorting to the following theory and assumptions (here detailed for only one particle):

(i) Without any applied field $\mathbf{E}_\infty$ and due to its interactions with the electrolyte, the surface S actually admits a charge distribution (for example of positive charges).

Consequently, the particle $\mathcal{P}$ is surrounded by a diffuse cloud $\mathcal{C}$ of counterions whose typical thickness is the Debye–Huckel screening length κ^{-1} (Anderson 1989). By counterions, one means negative (positive) ions for positive (respectively negative) charges on $\mathcal{S}$. The outer boundary of $\mathcal{C}$ is denoted by $\mathcal{S}^+$. Outside the double-layer $\mathcal{S} \cup \mathcal{C}$ the electrostatic potential or field and the charge density quickly vanish and both the electrolyte and the particle are motionless. Finally, one introduces the so-called zeta potential ζ (Hiemenz and Rajagopalan 1986) as the electrostatic potential on S in such circumstances (for a zero external field $\mathbf{E}_\infty$).

(ii) For a weak enough applied electric field $\mathbf{E}_\infty$ the previous charge distributions remain unchanged. However, those charges do modify the external field and we denote by ϕ and $\mathbf{E} = \mathbf{E}_\infty - \nabla\phi$ the perturbation potential and the electric field in the fluid domain. The field $\mathbf{E}$ induces a body force in the cloud $\mathcal{C}$ and a fluid flow. By viscosity the solid particle $\mathcal{P}$ thereafter experiences a rigid-body motion $(\mathbf{U}, \boldsymbol{\omega})$ of unknown translational velocity $\mathbf{U}$ (the velocity of one point O attached to $\mathcal{P}$) and angular velocity $\boldsymbol{\omega}$.

(iii) Since particles of interest are micron size, the Reynolds number $\mathrm{Re} = VL/\nu$, scaled on the typical fluid velocity V and particule size L, is very small (ν is the kinematic viscosity). Thus, the quasi-static creeping motion equations apply to the electrolyte flow $(\mathbf{u}, p)$ where $\mathbf{u}$ and p respectively denote the fluid velocity and pressure. If $\Omega^+ = \mathbb{R}^3 \setminus (\mathcal{P} \cup \mathcal{C})$ designates the fluid domain the functions ϕ, p and $\mathbf{u}$ thereafter obey the equations

$$\nabla^2\phi = 0, \quad \mu\nabla^2\mathbf{u} = \nabla p, \quad \nabla\cdot\mathbf{u} = 0 \ \text{ in } \Omega^+ . \quad (1.1)$$

(iv) The typical radius of curvature of $\mathcal{S}$ is assumed ("thin" double-layer theory) to be large compared to the cloud thickness κ^{-1}. Thus, Ω^+ and $\mathcal{S}^+$ respectively collapse to $\Omega := \mathbb{R} \setminus (\mathcal{P} \cup \mathcal{S})$ and $\mathcal{S}$ and one prescribes boundary conditions for the perturbation potential and the fluid velocity $\mathbf{u}$ and pressure p on S. More precisely, provided that $\mathcal{S}$ is insulating, those boundary conditions read

$$[\nabla\phi\cdot\mathbf{n}](M) = [\mathbf{E}_\infty\cdot\mathbf{n}](M). \quad \text{on } \mathcal{S} \quad (1.2)$$

$$\mathbf{u}^s(M) = \mathbf{u}(M) - [\mathbf{U} + \boldsymbol{\omega}\wedge\mathbf{OM}] = -\epsilon[\zeta\mathbf{E}](M)/\mu. \quad \text{on } \mathcal{S} \quad (1.3)$$

where $\mathbf{n}$ designates the unit outwarding normal and $\mathbf{u}^s$ a "slip velocity" (Anderson 1989) which results from the electrically driven flow inside $\mathcal{C}$. The Neumann boundary condition (1.2) holds in the limit of a non-conducting particle, i.e. when the double-layer (here of vanishing thickness) do not admit charge tranfert across it. For further details, the reader is directed to Hunter (1981). The relation (1.3) is established within the limit $\mathrm{Re} \to 0$. Finally, the governing problem (1.1)–(1.3) for $(\phi, \mathbf{u}, p)$ is supplemented with the following far field behavior

Received 26 February 2001

A. Sellier
LMFA, Ecole Centrale de Lyon/UCBL,
69131 Ecully Cedex, France
e-mail: sellier@mecaflu.ec-lyon.fr

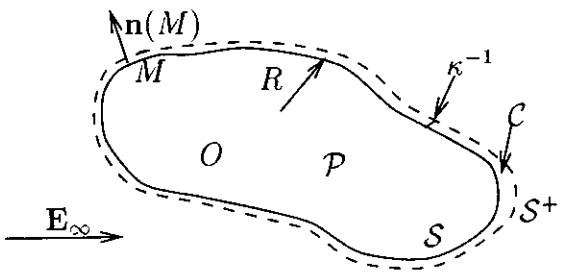

Fig. 1. A colloidal and charged particle embedded in the electric field $\mathbf{E}_\infty$

$$(\nabla\phi, \mathbf{u}(M), p(M)) \to (\mathbf{0}, \mathbf{0}, 0) \quad \text{as } AM \to \infty \,. \tag{1.4}$$

(v) Each particle is freely suspended. In addition, for a thin double-layer (assumption (iv)) the external electric field $\mathbf{E}_\infty$ applies zero net force and torque on each particle. Hence, the electrolyte flow produces no net hydrodynamic force and torque on any particle. For only one particle, these conditions read

$$\int_{\mathcal{S}} \boldsymbol{\sigma} \cdot \mathbf{n} \, dS = \mathbf{0}, \qquad \int_{\mathcal{S}} [\mathbf{OM} \wedge \boldsymbol{\sigma} \cdot \mathbf{n}] dS = \mathbf{0} \tag{1.5}$$

where $\boldsymbol{\sigma}$ denotes the usual Cauchy stress tensor, i.e. for our Newtonian electrolyte

$$\boldsymbol{\sigma} = -p\mathbf{1} + \mu(\nabla\mathbf{u} + {}^t\nabla\mathbf{u}) \,. \tag{1.6}$$

In determining $(\mathbf{U}, \boldsymbol{\omega})$ one usually proceeds as follows:

(i) First, obtain in the whole fluid domain Ω the perturbation potential ϕ and the electrolyte flow $(\mathbf{u}, p)$.
(ii) Finally, compute the stress tensor $\boldsymbol{\sigma}$ on the particle's surface $\mathcal{S}$ and deduce $(\mathbf{U}, \boldsymbol{\omega})$ by enforcing the conditions (1.5).

For a single particle of uniform zeta-potential ζ (one speaks of uniformly charged particle) embedded in a uniform electric field $\mathbf{E}_\infty$, such a treatment yields the celebrated Smoluchowski result

$$\mathbf{U} = \frac{\epsilon\zeta}{\mu}\mathbf{E}_\infty, \quad \boldsymbol{\omega} = \mathbf{0} \,. \tag{1.7}$$

Thus, the particle does not rotate and only translates along the direction of the applied field $\mathbf{E}_\infty$. This remarkable behavior has been first derived by Smoluchowski (1921) for a sphere and further extended to the case of an arbitrary shape by Morrison (1970) and Teubner (1982). The Smoluchowski equation (1.7) provides the very first approximation of the electrophoretic velocity of a dilute suspension of uniformly and equally charged particles embedded in a uniform electric field. However, determining the dependence of this velocity upon the weak particle concentration of a suspension of particles that present a distribution in both zeta potential and size at least requires to investigate the interaction effects between pair of particles. As achieved through a microscopic model by Anderson (1981) for identical spheres or Chen and Keh (1988) for spheres of unequal radii, such analysis indeed accounts for the volume-fraction effect on the average electrophorectic mobility in a bounded and dilute suspension of particles different both in size and uniform zeta potential. Accordingly, the interaction between two spheres has received a strong attention in the last two decades. For two identical spheres one can cite the pioneering work by Reed and Morrison (1976) that makes use of the bipolar coordinates but discards the allowed rotations of the spheres. The case of different spheres has been handled for a large center-to-center distance by a method of reflections by Chen and Keh (1988) and for any separation distance by Keh and Chen (1989a, b) by resorting again to the bipolar coordinates. For equal and uniform zeta potentials all these works found that the Smoluchowski solution (1.7) still holds: the two spheres translate (without rotation) at the same Smoluchowski's velocity. As established by Acrivos et al. (1990), this actually remains true for any number of identical spheres of the same and uniform zeta potential.

To the author's very best knowledge the case of two arbitrary particles of unequal and either uniform or non-uniform zeta potentials has not yet been addressed. As recently derived by Sellier (2001) two arbitrary particles admitting the same and uniform zeta potential experience the same Smoluchowski rigid-body motion (1.7) when embedded in a uniform electric field $\mathbf{E}_\infty$. For unequal potentials it is worth examining the interactions between the particles (and for uniformly charged surfaces the corrections to the Smoluchowski prediction) versus the separation distance, especially for near-contact particles. The aim of this work is to present a new and general approach that holds for arbitrary shapes, zeta potential functions and applied electric field $\mathbf{E}_\infty$. More precisely, the paper is organized as follows. Section 2 derives a key linear system that governs the two unknown rigid-body motions of the particles. Relevant boundary integral equations are established in Sect. 3. In Sect. 4 we detail the advocated numerical procedure and both present and discuss numerical benchmarks and new results for ellipsoids and spheroids. Finally, a few concluding remarks close the paper in Sect. 5.

2
The governing linear system

We consider two particles $\mathcal{P}_1$ and $\mathcal{P}_2$ of smooth enough boundaries $\mathcal{S}_1$ and $\mathcal{S}_2$ (see Fig. 2). The total surface $\mathcal{S}$ reads $\mathcal{S} = \mathcal{S}_1 \cup \mathcal{S}_2$ and the fluid domain is $\Omega = \mathbb{R}^3 \setminus (\mathcal{P}_1 \cup \mathcal{P}_2 \cup \mathcal{S})$. Henceforth, Cartesian coordinates (O, x_1, x_2, x_3) and the tensor summation convention are adopted whilst indices α or β belong to $\{1, 2\}$ and indices i, j or ν belong to $\{1, 2, 3\}$. Under these notations, ζ_α is the zeta potential of the surface $\mathcal{S}_\alpha$ and the particle $\mathcal{P}_\alpha$ experiences a rigid-body motion $(\mathbf{U}^{(\alpha)}, \boldsymbol{\omega}^{(\alpha)})$ of

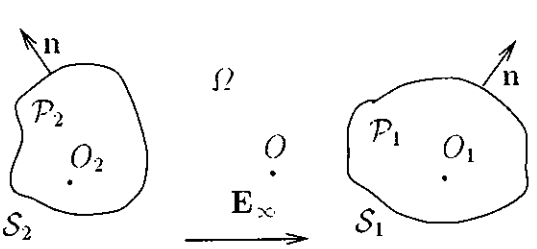

Fig. 2. Our notations for two particles $\mathcal{P}_1$ and $\mathcal{P}_2$

unknown velocity components $U_i^{(\alpha)} = \mathbf{U}^{(\alpha)} \cdot \mathbf{e}_i$ and $\omega_i^{(\alpha)} = \boldsymbol{\omega}^{(\alpha)} \cdot \mathbf{e}_i$.

According to the previous section, in such circumstances the perturbation potential ϕ fulfills the well-posed and exterior Neumann-type problem

$$\nabla\phi = 0 \text{ in } \Omega, \quad \nabla\phi \to 0 \text{ as } r \to \infty \ , \tag{2.1}$$

$$\nabla\phi \cdot \mathbf{n} = \mathbf{E}_\infty \cdot \mathbf{n} \quad \text{on } \mathcal{S} \tag{2.2}$$

where $r := OM$. If O_α designates a given point attached to $\mathcal{P}_\alpha$, inspecting the boundary condition (1.3) we define the velocity field $\mathbf{u}_d$ as

$$\mathbf{u}_d(M) = \mathbf{U}^{(\alpha)} + \boldsymbol{\omega}^{(\alpha)} \wedge \mathbf{O}_\alpha\mathbf{M} - \left[\frac{\epsilon\zeta_\alpha \mathbf{E}}{\mu}\right](M) \quad \text{on } \mathcal{S}_\alpha \tag{2.3}$$

and the electrolyte flow $(\mathbf{u}, p)$ obeys the following equations

$$\mu\nabla^2\mathbf{u} = \nabla p; \quad \nabla \cdot \mathbf{u} = 0 \text{ in } \Omega \ , \tag{2.4}$$

$$(\mathbf{u}, p) \to (\mathbf{0}, 0) \text{ as } r \to \infty \quad \text{and} \quad \mathbf{u} = \mathbf{u}_d \text{ on } \mathcal{S} \ . \tag{2.5}$$

As previously suggested, one might deduce the required rigid-body motions $(\mathbf{U}^{(1)}, \boldsymbol{\omega}^{(1)})$ and $(\mathbf{U}^{(2)}, \boldsymbol{\omega}^{(2)})$ by expressing from (2.1)–(2.5) the functions ϕ, p and $\mathbf{u}$ in the whole fluid domain Ω and the stress tensor $\boldsymbol{\sigma}$ on $\mathcal{S}$ in terms of our twelve unknown velocity components $U_i^{(\alpha)}$ or $\omega_i^{(\alpha)}$ and thereafter enforcing the counterpart of (1.5), i.e. the twelve conditions

$$\int_{\mathcal{S}_\alpha} \mathbf{e}_i \cdot \boldsymbol{\sigma} \cdot \mathbf{n}\, d\mathcal{S}_\alpha = 0, \quad \int_{\mathcal{S}_\alpha} [\mathbf{e}_i \wedge \mathbf{O}_\alpha\mathbf{M}] \cdot \boldsymbol{\sigma} \cdot \mathbf{n}\, d\mathcal{S}_\alpha = 0 \ . \tag{2.6}$$

With the notable exception of the two-sphere cluster (for which the use of bipolar coordinates succeeded in providing analytical results) only a numerical treatment seems thinkable for arbitrary particles and calculating ϕ, p and $\mathbf{u}$ in the whole unbounded domain Ω (for instance by resorting to Finite Elements) results in a costly computing challenge. Thus, it is highly desirable to look at a whole boundary formulation. In this paper this is achieved in two steps:

Step 1. Prove, in this section, that one only needs to compute a few number of relevant quantities on the surface $\mathcal{S}$.

Step 2. Show, in the next Sect. 3, that it is actually possible to obtain those required surface quantities by solving boundary integral equations on the bounded surface $\mathcal{S}$.

The first step rests on the exploitation of the well-known Lorentz reciprocal identity for Stokes flow. For two arbitrary Stokes flows $(\mathbf{u}, p)$ and $(\mathbf{u}', p')$ of stress tensors $\boldsymbol{\sigma}(\mathbf{u}, p)$ and $\boldsymbol{\sigma}'(\mathbf{u}', p')$ and subject to the equations (2.4)–(2.5), respectively for boundary conditions $\mathbf{u}_d$ and $\mathbf{u}'_d$, the following relation holds, on the surface $\mathcal{S}$,

$$\int_{\mathcal{S}} \mathbf{u}'_d \cdot \boldsymbol{\sigma}(\mathbf{u}, p) \cdot \mathbf{n}\, d\mathcal{S} = \int_{\mathcal{S}} \mathbf{u}_d \cdot \boldsymbol{\sigma}'(\mathbf{u}', p') \cdot \mathbf{n}\, d\mathcal{S} \ . \tag{2.7}$$

Note that the establishment of (2.7) makes use of the good decay of $(\mathbf{u}, p)$ and $(\mathbf{u}', p')$ at infinity; functions $\mathbf{u}$ and p respectively behaving like $1/r$ and $1/r^2$ (see, for instance, Kim and Karrila 1991). At this stage it is fruitful to introduce twelve specific Stokes flows $(\mathbf{u}_T^{(k),i}, p_T^{(k),i})$ and $(\mathbf{u}_R^{(k),i}, p_R^{(k),i})$ that obey the creeping motion equations (2.4), the far-field behavior (2.5) and the boundary conditions

$$\mathbf{u}_T^{(\alpha),i} = \delta_{\alpha\beta}\mathbf{e}_i, \quad \mathbf{u}_R^{(\alpha),i} = \delta_{\alpha\beta}[\mathbf{e}_i \wedge \mathbf{O}_\alpha\mathbf{M}] \text{ on } \mathcal{S}_\beta \tag{2.8}$$

where δ designates the Kronecker delta. Clearly, one particle is motionless whereas the other one admits a unit translation or rotation in the $\mathbf{e}_i$ direction (with letters T and R respectively for the translation or the rotation). For $L \in \{T, R\}$, $\mathbf{f}_L^{(\alpha),i} = \boldsymbol{\sigma}(\mathbf{u}_L^{(\alpha),i}, p_L^{(\alpha),i})\mathbf{n}$ designates the surface forces that arise on $\mathcal{S}$ for these specific Stokes flows of the electrolyte. By successively selecting each specific Stokes flow for $(\mathbf{u}', p')$ in applying the key relation (2.7), it is possible to cast any condition (2.6) into a more pleasant form. For example, note that

$$\begin{aligned}
&\int_{\mathcal{S}_\alpha} \mathbf{e}_i \cdot \boldsymbol{\sigma}(\mathbf{u}, p) \cdot \mathbf{n}\, d\mathcal{S}_\alpha \\
&= \int_{\mathcal{S}} \mathbf{u}_T^{(\alpha),i} \cdot \boldsymbol{\sigma}(\mathbf{u}, p) \cdot \mathbf{n}\, d\mathcal{S} \\
&= \int_{\mathcal{S}_1} \mathbf{u}_d \cdot \mathbf{f}_T^{(\alpha),i}\, d\mathcal{S}_1 + \int_{\mathcal{S}_2} \mathbf{u}_d \cdot \mathbf{f}_T^{(\alpha),i}\, d\mathcal{S}_2 \ .
\end{aligned} \tag{2.9}$$

In virtue of our Def. (2.3), the zero net hydrodynamic force conditions in (2.6) thereafter become

$$\begin{aligned}
\int_{\mathcal{S}} \frac{\epsilon\zeta\mathbf{E}}{\mu} \cdot \mathbf{f}_T^{(\alpha),i}\, d\mathcal{S} &= \int_{\mathcal{S}_1} [\mathbf{U}^{(1)} + \boldsymbol{\omega}^{(1)} \wedge \mathbf{O}_1\mathbf{M}] \cdot \mathbf{f}_T^{(\alpha),i}\, d\mathcal{S}_1 \\
&\quad + \int_{\mathcal{S}_2} [\mathbf{U}^{(2)} + \boldsymbol{\omega}^{(2)} \wedge \mathbf{O}_2\mathbf{M}] \cdot \mathbf{f}_T^{(\alpha),i}\, d\mathcal{S}_2 \ .
\end{aligned} \tag{2.10}$$

By using the specific flows $(\mathbf{u}_R^{(\alpha),i}, p_R^{(\alpha),i})$, other conditions prescribed by (2.6) are treated in a similar fashion. Finally, one arrives at the following linear system of twelve equations, for the unknown velocity components $U_j^{(\alpha)} = \mathbf{U}^{(\alpha)} \cdot \mathbf{e}_j$ and $\boldsymbol{\omega}_j^{(\alpha)} = \boldsymbol{\omega}^{(\alpha)} \cdot \mathbf{e}_j$,

$$A_{(\alpha).T}^{(1).ij} U_j^{(\alpha)} + B_{(\alpha).T}^{(1).ij} \boldsymbol{\omega}_j^{(\alpha)} = \frac{\epsilon}{\mu} \int_{\mathcal{S}} \zeta\mathbf{E} \cdot \mathbf{f}_T^{(1),i}\, d\mathcal{S} \ . \tag{2.11}$$

$$A_{(\alpha).T}^{(2).ij} U_j^{(\alpha)} + B_{(\alpha).T}^{(2).ij} \boldsymbol{\omega}_j^{(\alpha)} = \frac{\epsilon}{\mu} \int_{\mathcal{S}} \zeta\mathbf{E} \cdot \mathbf{f}_T^{(2),i}\, d\mathcal{S} \ . \tag{2.12}$$

$$A_{(\alpha).R}^{(1).ij} U_j^{(\alpha)} + B_{(\alpha).R}^{(1).ij} \boldsymbol{\omega}_j^{(\alpha)} = \frac{\epsilon}{\mu} \int_{\mathcal{S}} \zeta\mathbf{E} \cdot \mathbf{f}_R^{(1),i}\, d\mathcal{S} \ . \tag{2.13}$$

$$A_{(\alpha).R}^{(2).ij} U_j^{(\alpha)} + B_{(\alpha).R}^{(2).ij} \boldsymbol{\omega}_j^{(\alpha)} = \frac{\epsilon}{\mu} \int_{\mathcal{S}} \zeta\mathbf{E} \cdot \mathbf{f}_R^{(2),i}\, d\mathcal{S} \ . \tag{2.14}$$

where arising coefficients obey, for $L \in \{T, R\}$,

$$A^{(\beta),i,j}_{(\alpha),L} = \int_{\mathcal{S}_\alpha} \mathbf{e}_j \cdot \mathbf{f}_L^{(\beta),i}\, \mathrm{d}S_\alpha \ , \tag{2.15}$$

$$B^{(\beta),i,j}_{(\alpha),L} = \int_{\mathcal{S}_\alpha} (\mathbf{e}_j \wedge \mathbf{O}_\alpha\mathbf{M}) \cdot \mathbf{f}_L^{(\beta),i}\, \mathrm{d}S_\alpha \ . \tag{2.16}$$

For example, the relation (2.10) readily follows from the Eq. (2.11), for any integer i in $\{1,2,3\}$. Hence, the generalized unknown velocity $X = (U_j^{(1)}, U_j^{(2)}, \omega_j^{(1)}, \omega_j^{(2)})$ obeys the system (2.11)–(2.14) of twelve linear and algebraic equations. The associated 12×12 square matrix $\mathbf{M}$ is termed the grand resistance matrix (see Kim and Karrila 1991). As proved in Happel and Brenner (1973), this matrix $\mathbf{M}$ is symmetric and negative-definite. Thereby, the system (2.11)–(2.14) admits a unique solution.

Keeping in mind that $\mathbf{E} = \mathbf{E}_\infty - \nabla\phi$, a straightforward inspection of our system and definitions (2.15)–(2.16) immediately reveals that one needs to compute the vectors $\nabla\phi$ and $\mathbf{f}_L^{(\beta),i}$ on the surface $\mathcal{S}$ only in getting the unique generalized velocity X. This nice feature strongly suggests to look at a boundary formulation that would directly provide those quantities on $\mathcal{S}$. As the next Section shows, this is indeed possible to calculate the required quantities $\nabla\phi$ and $\mathbf{f}_L^{(\beta),i}$ on $\mathcal{S}$ by solving thirteen boundary integral equations. As a consequence and contrary to previous works in the field, it is no use computing the perturbation potential ϕ and the electrolyte flow $(\mathbf{u}, p)$ in the whole fluid domain Ω.

3
The relevant boundary integral equations

This section presents the boundary integral equations of interest for the proposed approach.

3.1
Getting the vector $\nabla\phi$ on $\mathcal{S}$

The perturbation potential ϕ obeys the problem (2.1)–(2.2). As the boundary condition (2.2) provides the normal derivative of ϕ, the question actually reduces to the numerical approximation of the tangential derivatives of ϕ on the surface $\mathcal{S}$. Here, this is achieved by first computing the function ϕ on $\mathcal{S}$ (as the numerical solution of a boundary integral equation) and thereafter building a numerical estimation of the required tangential derivatives. More precisely, from (2.1)–(2.2) the boundary value of the perturbation potential is easily found to satisfy the well-known Fredholm boundary integral equation of the second kind

$$-4\pi\phi(M) + \int_{\mathcal{S}} [\phi(P) - \phi(M)] \frac{\mathbf{PM}\cdot\mathbf{n}(P)}{PM^3}\, \mathrm{d}S$$

$$= \int_{\mathcal{S}} \frac{[\mathbf{E}_\infty \cdot \mathbf{n}](P)}{PM}\, \mathrm{d}S \ . \tag{3.1}$$

If $\mathcal{H}^s(\mathcal{S})$ denotes the usual Sobolev space, this well-posed integral equation admits a unique solution in $\mathcal{H}^{-1/2}(\mathcal{S})$ as soon as $\mathbf{E}_\infty \cdot \mathbf{n} \in \mathcal{H}^{-1/2}(\mathcal{S})$ (see Dautray and Lions 1988).

3.2
Getting the surface forces $\mathbf{f}_L^{(\beta),i}$ on $\mathcal{S}$

For an arbitrary velocity data $\mathbf{u}_d$ the Stokes flow $(\mathbf{u}, p)$ solution to (2.4)–(2.5) is unique (Ladyzenskaya 1969). In addition, for any point M of the fluid domain Ω (see, for instance, Pozrikidis 1992) the following representation holds

$$u_j(M) = -\frac{1}{8\pi\mu}\int_{\mathcal{S}} f_i(P) G_{ij}(P,M)\mathrm{d}S + \frac{1}{8\pi}\int_{\mathcal{S}} u_i(P) T_{ijv}(P,M)[\mathbf{n}\cdot\mathbf{e}_v](P)\mathrm{d}S \tag{3.2}$$

where $v \in \{1,2,3\}$, $u_j = \mathbf{u}\cdot\mathbf{e}_j$, $f_i = \mathbf{e}_i.\boldsymbol{\sigma}\cdot\mathbf{n}$ and the Oseen tensor $\mathbf{G} = G_{ij}\mathbf{e}_i \otimes \mathbf{e}_j$ and the stress tensor $\mathbf{T} = T_{ijv}\mathbf{e}_i \otimes \mathbf{e}_j \otimes \mathbf{e}_v$ are given explicitly by

$$G_{ij}(P,M) = \frac{\delta_{ij}}{PM} + \frac{(\mathbf{PM}\cdot\mathbf{e}_i)(\mathbf{PM}\cdot\mathbf{e}_j)}{PM^3} \ , \tag{3.3}$$

$$T_{ijv}(P,M) = 6\frac{(\mathbf{PM}\cdot\mathbf{e}_i)(\mathbf{PM}\cdot\mathbf{e}_j)(\mathbf{PM}\cdot\mathbf{e}_v)}{PM^5} \ . \tag{3.4}$$

The first and the second integral occurring in (3.2) are respectively termed the single-layer and the double-layer distribution. Now we consider any rigid-body motion $\mathbf{U} + \boldsymbol{\omega}\wedge\mathbf{O}_\beta\mathbf{M}$ of the same electrolyte in the interior of the particle $\mathcal{P}_\beta$. Such a bounded flow is actually a Stokes flow of constant pressure p and stress tensor $\boldsymbol{\sigma} = -p\mathbf{1}$. Any point M of the fluid domain Ω is located outside the interior of $\mathcal{P}_l$ and thereafter (see Eq. (2.3.4) in Pozrikidis 1992) one obtains

$$0 = \int_{\mathcal{S}_\beta} ([\mathbf{U} + \boldsymbol{\omega}\wedge\mathbf{O}_\beta\mathbf{P}]\cdot\mathbf{e}_i) T_{ijv}(P,M)[\mathbf{n}\cdot\mathbf{e}_v](P)\mathrm{d}S_\beta - \frac{p}{\mu}\int_{\mathcal{S}_\beta} n_i(P) G_{ij}(P,M)\mathrm{d}S_\beta \ . \tag{3.5}$$

Because the Oseen tensor $\mathbf{G}$ is divergence free, the last integral arising on the right-hand side of (3.5) actually vanishes for any location of the point M. In other words, the key identity

$$\int_{\mathcal{S}_\beta} n_i(P) G_{ij}(P,M)\mathrm{d}S_\beta = 0 \tag{3.6}$$

holds for a point M located outside the particle $\mathcal{P}_\beta$, right on the surface $\mathcal{S}_\beta$ or inside the particle. Thus, for any rigid-body $\mathbf{U} + \boldsymbol{\omega}\wedge\mathbf{O}_\beta\mathbf{M}$ one obtains, for M lying in the fluid domain Ω,

$$\int_{\mathcal{S}_\beta} ([\mathbf{U} + \boldsymbol{\omega}\wedge\mathbf{O}_\beta\mathbf{P}]\cdot\mathbf{e}_i) T_{ijv}(P,M)[\mathbf{n}\cdot\mathbf{e}_v](P)\mathrm{d}S_\beta = 0 \ . \tag{3.7}$$

Accordingly, for any specific Stokes flow $(\mathbf{u}_L^{(\alpha),i}, p_L^{(\alpha),i})$ that satisfies a rigid-body motion type boundary condition on $\mathcal{S}_1$ and $\mathcal{S}_2$ (see (2.8)) the double-layer term arising in (3.2) vanishes and the velocity representation becomes

$$\mathbf{e}_j \cdot u_L^{(\alpha),i}(M) = -\frac{1}{8\pi\mu}\int_S [\mathbf{f}_L^{(\alpha),i}](P)\cdot \mathbf{e}_v G_{vj}(P,M)\mathrm{d}S \tag{3.8}$$

One thereafter speaks of single-layer representation for our twelve specific Stokes flow in the fluid domain Ω. Since this single-layer is actually continuous as the point M crosses the boundary S, the Eq. (3.8) is also valid on the boundary $S_1 \cup S_2$. This remark immediately yields the Fredholm boundary integral equations of the first kind

$$\int_S \left\{\frac{\delta_{jv}}{PM} + \frac{(\mathbf{PM}\cdot\mathbf{e}_j)(\mathbf{PM}\cdot\mathbf{e}_v)}{PM^3}\right\}\left[\frac{\mathbf{f}_L^{(\alpha),i}\cdot\mathbf{e}_v}{8\pi\mu}\right](P)\mathrm{d}S = [\mathbf{u}_L^{(\alpha),i}\cdot\mathbf{e}_j](M) \quad \text{for} \quad M \quad \text{on} \quad S\ . \tag{3.9}$$

Those integral equations govern the required surface tractions $\mathbf{f}_L^{(\alpha),i}$ on S for our twelve specific Stokes flows. At this stage, the existence and uniqueness of solution of (3.9) become of theoretical importance. Multiplying (3.9) on any surface S_β by the normal vector $\mathbf{n}$, integrating on S_β and switching the integrations on S and S_β, and finally exploiting the identity (3.6) easily yields the integral constraints for the right-hand side of (3.9)

$$\int_{S_\beta} [\mathbf{u}_L^{(\alpha),i}\cdot\mathbf{n}]\mathrm{d}S_\beta = 0, \quad l \in \{1,2\}\ . \tag{3.10}$$

Prescribed boundary conditions (2.8) actually ensure that those constraints are met for our specific Stokes flow and it is worth investigating the existence of eigensolutions $\mathbf{q}$ of the corresponding homogeneous integral equation, i.e such that

$$\int_S [\mathbf{q}\cdot\mathbf{e}_v](P)G_{vj}(P,M)\mathrm{d}S = 0, \quad \text{for } M \text{ on } S\ . \tag{3.11}$$

In virtue of (3.6), for any constant and real values λ_1 and λ_2 the function $\mathbf{q}(\lambda_1,\lambda_2)$ defined as

$$\mathbf{q}(\lambda_1,\lambda_2) = \lambda_1\mathbf{n} \text{ on } S_1. \quad \mathbf{q}(\lambda_1,\lambda_2) = \lambda_2\mathbf{n} \text{ on } S_2\ , \tag{3.12}$$

is an eigensolution. Conversely, arguments similar to those invoked by Pozrikidis (1992) in the case of a simply-connected surface S show that any eigensolution is of the present form (3.12). In summary, each integral equation (3.9) admits an infinity of solutions $\mathbf{f}_L^{(\alpha),i} = \mathbf{g}_L^{(\alpha),i} + \mathbf{q}(\lambda_1,\lambda_2)$ where $\mathbf{g}_L^{(\alpha),i}$ denotes any particular solution. However, the special form (3.12) of any eigenfunction $\mathbf{q}(\lambda_1,\lambda_2)$ together with the enforced boundary condition (2.2) ensure that the right-hand sides of our governing system (2.11)–(2.14), its associated matrix $\mathbf{M}$ (inspect definitions (2.15)–(2.16)) and thereby its unique solution $X = (U_j^{(1)}, U_j^{(2)}, \omega_j^{(1)}, \omega_j^{(2)})$ do not depend upon the choice of the selected solutions $\mathbf{f}_L^{(\alpha),i}$.

4
Numerical strategy and numerical results

As previously outlined, the general case of two particles of arbitrary shapes and configurations imposes to resort to a numerical treatment. This section first presents a numerical method without restriction on the shapes and configurations of the particles and finally both gives and discusses numerical results for two ellipsoids of uniform zeta potentials.

4.1
A boundary element method

Our thirteen boundary integral equations (3.1) and (3.9) are discretized by using an isoparametric boundary element method: each unknown is interpolated on S from a finite set of boundary values at the nodes of a surface mesh. We briefly describe the main steps of the procedure implementation and refer the reader for further details to the standard textbooks (see, among others, Brebbia 1994, Beskos 1987 and Bonnet 1999).

Step 1. Discretize each surface S_α into $N_e(\alpha)$ six-node triangular and curvilinear boundary elements $\Delta_e^{(\alpha)}$ with $e \in \{1,\ldots,N_e(\alpha)\}$. This is achieved by using a $N_d(\alpha)$-node mesh on S_α and each boundary element $\Delta_e^{(\alpha)}$ is mapped to the standard triangle Δ of inequations $0 \le \xi_1 \le 1$, $0 \le \xi_2 \le 1$ and $\xi_1 + \xi_2 \le 1$ in plane Cartesian and intrinsic coordinates $\xi = (\xi_1,\xi_2)$ by the following six quadratic shape functions M_q defined, for $q \in \{1,\ldots,6\}$ and $\xi_3 := 1 - \xi_1 - \xi_2$, as

$$M_1(\xi) = (2\xi_3 - 1)\xi_3, \quad M_2(\xi) = 4\xi_1\xi_3\ , \tag{4.1}$$

$$M_3(\xi) = (2\xi_1 - 1)\xi_1, \quad M_4(\xi) = 4\xi_1\xi_2\ , \tag{4.2}$$

$$M_5(\xi) = (2\xi_2 - 1)\xi_2, \quad M_6(\xi) = 4\xi_2\xi_3\ . \tag{4.3}$$

Accordingly, each boundary element $\Delta_e^{(\alpha)}$ is characterized by its six nodes $Y_\alpha^{(e.q)}$ (three corners and three midsides) and any point $P(\xi)$ on $\Delta_e^{(\alpha)}$, of intrinsic coordinates ξ, is given by

$$\mathbf{O}_\alpha\mathbf{P}(\xi) = \sum_{q=1}^{6} M_q(\xi)\mathbf{O}_\alpha\mathbf{Y}_\alpha{}^{(e.q)}\ . \tag{4.4}$$

Step 2. Each integral equation of unknown quantity F is evaluated at any node $M(n)$ with $1 \le n \le N_d(1) + N_d(2)$. If F_l denotes the restriction of F to S_l, one has to approximate in any case the following integral

$$I_\alpha[M(n)] = \int_{S_\alpha} F_\alpha(P)K[P,M(n)]\mathrm{d}S_\alpha \tag{4.5}$$

where K is a kernel of $1/PM$ type weak singularity. The previous boundary discretization of S_α and the isoparametric interpolation

$$F_\alpha[P(\xi)] = \sum_{q=1}^{6} M_q(\xi)F_\alpha^{(e.q)},\ F_\alpha^{(e.q)} := F_\alpha[Y_\alpha^{(e.q)}] \tag{4.6}$$

of F_α on S_α readily yield

$$I_\alpha[M(n)] = \sum_{e=1}^{N_e(\alpha)}\sum_{q=1}^{6} C_\alpha^{(e.q)}[M(n)]F_\alpha^{(e.q)}\ . \tag{4.7}$$

$$C_\alpha^{(e.q)}[M(n)] = \int_{\Delta_e^{(\alpha)}} K[\xi, M(n)][M_q J^{(\alpha)}](\xi)\mathrm{d}\xi\ . \tag{4.8}$$

where $J^{(\alpha)}$ designates the Jacobian of the mapping (4.4) from our Cartesian coordinates $x_i(P) = \mathbf{OP} \cdot \mathbf{e}_i$ to the intrinsic coordinates ξ. Gaussian integration formulas established by Lyness and Jespersen (1975) are employed in approximating each integral $C_\alpha^{(e,q)}[M(n)]$ with two different circumstances:

(i) If our node $M(n)$ lies on the boundary element $\Delta_e^{(\alpha)}$, the encountered weak singularity is removed by resorting to polar coordinates in the space of intrinsic coordinates ξ (see Bonnet 1999).

(ii) If $M(n)$ lies outside $\Delta_e^{(\alpha)}$ the regular integral $C_\alpha^{(e,q)}[M(n)]$ is computed by using more or less refined Gauss integration formulas (the chosen formulas depend upon a "severity" parameter that takes into account the distance from the boundary element (see Rezahat et al. 1986).

Step 3. If $N_d = N_d(1) + N_d(2)$ each integral equation thereafter becomes a linear system $\mathbf{AX} = \mathbf{Y}$ of fully populated and non-symmetric square $N_d \times N_d$ (for Eq. (3.1)) or $3N_d \times 3N_d$ (for Eqs. (3.9)) influence matrix $\mathbf{A}$. For our two-particle cluster it is possible to store the matrix $\mathbf{A}$. Thus, each system $\mathbf{AX} = \mathbf{Y}$ is solved by resorting to a standard LU factorization algorithm (subroutines DGETRF and DGETRS of the Lapack Library).

This procedure is quite suitable for the integral equation (3.1) which is of the second kind and admits a unique solution. As highlighted by our theoretical analysis of Sect. 3.2, the integral equations (3.9) do not have a unique solution and this suggests numerical troubles. On a theoretical ground we face with ill-conditioned boundary integral equations of the first kind but in practice this ill-posedness is not apparent unless very fine meshes are used (see Tran-Cong and Phan-Thien 1989; Pozrikidis 1992): the computed influence matrix $\mathbf{A}$ associated to the discretized boundary equations (3.9) is nonsingular.

Finally any surface integration that occurs in calculating the matrix $\mathbf{M}$ and the right-hand sides of our system (2.11)–(2.14) is performed with seven Gauss points on each boundary element $\Delta_e^{(\alpha)}$.

The proposed boundary element method holds for any particles shapes and configurations: one only needs a mesh for any surface $\mathcal{S}_\alpha$. Henceforth, we actually restrict our attention to the case of two ellipsoids. More precisely, each surface $\mathcal{S}_\alpha$ admits the equation

$$\frac{x_1^2}{a_l^2} + \frac{x_2^2}{b_l^2} + \frac{[x_3 - x_3(l)]^2}{c_l^2} = 1 \ . \tag{4.9}$$

with $\mathbf{OO}_\alpha = x_3(\alpha)\mathbf{e}_3$. Thus, the vector $\mathbf{e}_3$ is directed along the line of centers O_1 and O_2. The center-to-center distance $d = O_1O_2$ equals $c_1 + c_2$ for touching particles and is greater than $c_1 + c_2$ for separated ellipsoids. For elliptical angles $\theta_\alpha \in [0, 2\pi]$ and $\varphi_\alpha \in [0, \pi]$ such that

$$x_1 = a_l \sin\varphi_\alpha \cos\theta_\alpha . x_2 = b_\alpha \sin\varphi_\alpha \sin\theta_\alpha \ . \tag{4.10}$$

$$x_3 - x_3(\alpha) = c_\alpha \cos\varphi_\alpha \tag{4.11}$$

we discretize $\mathcal{S}_\alpha$ by employing the following two-parameter $N_d(\alpha)$ - node mesh of $N_e(\alpha)$ boundary elements (characterized by two positive integers $E(\alpha)$ and $N_\varphi(\alpha) \geq 3$))

$$\theta_\alpha = 2\pi(\alpha_\theta - 1)/N_\theta(\alpha), \quad \varphi_\alpha = \pi\alpha_\varphi/[2N_\varphi(\alpha)] \ , \tag{4.12}$$

$$N_\theta(\alpha) = 12 \times 2^{E(\alpha)} \tag{4.13}$$

for positive integers α_θ and α_φ that obey the conditions

$$1 \leq \alpha_\theta \leq N_\theta(\alpha) \quad \text{if } 2 \leq \alpha_\varphi \leq 2[N_\varphi(\alpha) - 1] \ , \tag{4.14}$$

$$\frac{\alpha_\theta}{2} = k \in \left\{0, \ldots, \frac{N_\theta(\alpha)}{2} - 1\right\}, \quad \alpha_\varphi \in \{1, 2N_\varphi(\alpha) - 1\} \ . \tag{4.15}$$

Under this choice, one immediately obtains

$$N_d(\alpha) = 2\{1 + N_\theta(\alpha)[N_\varphi(\alpha) - 1]\} \ . \tag{4.16}$$

$$N_e(\alpha) = N_\theta(\alpha)[N_\varphi(\alpha) - 1], \quad N_\theta(\alpha) = 12 \times 2^{E(\alpha)} \ . \tag{4.17}$$

Henceforth, the notation $N_d(\alpha) = [N_\varphi(\alpha), E(\alpha)]$ means that (4.16)–(4.17) hold.

4.2 Numerical comparisons

In this whole subsection the external field $\mathbf{E}_\infty$ and the zeta potentials ζ_1 and ζ_2 are uniform. Two benchmarks are proposed.

(i) The case $\zeta_1 = \zeta_2$. In such circumstances, each charged ellipsoid experiences the Smoluchowski rigid-body translation (1.7) whatever the separation distance d! This theoretical result, first obtained for any number of identical spheres by Acrivos et al. (1990) and recently extended by Sellier (2001) to the case of arbitrary shapes, provides a nice numerical test. We set $\zeta_1 = \zeta_2 = \zeta \neq 0$, impose $\mathbf{E}_\infty = \mathbf{e}_1 + \mathbf{e}_2 + \mathbf{e}_3$ and look at the electrophoretic mobilities

$$u_i^{(\alpha)} := \frac{\mu[\mathbf{U}^{(\alpha)} \cdot \mathbf{e}_i]}{\epsilon\zeta[\mathbf{E}_\infty \cdot \mathbf{e}_i]}, \quad v_i^{(\alpha)} := r_\alpha \frac{\mu[\boldsymbol{\omega}^{(\alpha)} \cdot \mathbf{e}_i]}{\epsilon\zeta[\mathbf{E}_\infty \cdot \mathbf{e}_i]} \ , \tag{4.18}$$

where $r_\alpha = \max(a_\alpha, b_\alpha, c_\alpha)$. Theoretical results predict that $u_i^{(\alpha)} = 1$ and $v_i^{(\alpha)} = 0$ for any center-to-center distance d. In Table 1a–c we list the computed values of $u_i^{(\alpha)}$ for two ellipsoids defined by $a_1 = 1.2, b_1 = 0.8, c_1 = 1.0, a_2 = 0.8, b_2 = 1.0$ and $c_2 = 1.2, x_3(2) = 0$ and $d = x_3(1) > 2.2$. In this case $d \geq 2.2$. For only 74 collocation points on any surface $\mathcal{S}_\alpha$, a one percent accuracy is observed in the whole range $d \geq 2.4$. For $d \geq 5$, the numerical errors, incurred by these surface meshes, do not depend on d. As expected, for close particles (as soon as the distance between particle surfaces becomes comparable to our mesh size) the accuracy both depends on d and deteriorates. As indicated in Table 1b,c, the use of more and more refined $N_d(\alpha)$-node surface meshes makes it possible to obtain, if required, excellent approximations of each electrophoretic mobility $u_i^{(\alpha)}$.

As shown in Table 2, similar trends are obtained for the mobilities $v_i^{(\alpha)}$. The use of 74-node surface meshes yields a one percent accuracy.

(ii) The case $\zeta_1 \neq \zeta_2$. In virtue of (2.1)–(2.2), the resulting electric field $\mathbf{E}$ is a linear function of $\mathbf{E}_\infty$. Using the decompositions

Table 1. Computed mobilities $u_i^{(\alpha)}$ for two ellipsoids with $a_1 = 1.2$, $b_1 = 0.8$, $c_1 = 1.0$, $a_2 = 0.8$, $b_2 = 1.0$, $c_2 = 1.2$ and $x_3(2) = 0$, $d = x_3(1) > 2.2$

d	$u_1^{(1)}$	$u_2^{(1)}$	$u_3^{(1)}$	$u_1^{(2)}$	$u_2^{(2)}$	$u_3^{(2)}$
(a) Case $N_d(1) = N_d(2) = 74 = [4, 0]$						
2.4	1.0076	1.0110	1.0059	1.0136	1.0071	1.0084
5	1.0087	1.0095	1.0077	1.0112	1.0076	1.0063
10	1.0087	1.0096	1.0076	1.0113	1.0077	1.0063
(b) Case $N_d(1) = N_d(2) = 242 = [6, 1]$						
2.3	1.0003	1.0024	0.9995	1.0030	1.0010	1.0018
2.4	1.0005	1.0011	1.0004	1.0015	1.0007	1.0011
5	1.0008	1.0009	1.0007	1.0009	1.0007	1.0007
10	1.0008	1.0009	1.0006	1.0009	1.0007	1.0006
30	1.0008	1.0009	1.0006	1.0009	1.0007	1.0006
100	1.0008	1.0009	1.0006	1.0009	1.0007	1.0006
(c) Case $N_d(1) = N_d(2) = 434 = [10, 1]$						
2.3	1.0002	1.0005	1.0002	1.0008	1.0003	1.0005
2.4	1.0002	1.0003	1.0003	1.0004	1.0002	1.0004
5	1.0002	1.0003	1.0003	1.0004	1.0002	1.0004
10	1.0002	1.0003	1.0003	1.0004	1.0002	1.0004

$$\zeta_\alpha = \frac{\zeta_1 + \zeta_2}{2} + (-1)^{\alpha+1}\frac{\zeta_1 - \zeta_2}{2} \quad , \tag{4.19}$$

the previous extension of the Smoluchowski solution for particles of the same and uniform zeta potentials $(\zeta_1 + \zeta_2)/2$ and inspecting the governing system (2.11)–(2.14) reveals that

$$\mathbf{U}^{(\alpha)} = \frac{\epsilon}{\mu}\left[\frac{\zeta_1 + \zeta_2}{2}\mathbf{1} + (-1)^\alpha\frac{\zeta_1 - \zeta_2}{2}(2\mathbf{I}_T^{(\alpha)} - \mathbf{1})\right]\cdot\mathbf{E}_\infty \quad , \tag{4.20}$$

$$\boldsymbol{\omega}^{(\alpha)} = \frac{(-1)^\alpha\epsilon}{\mu}(\zeta_1 - \zeta_2)\mathbf{I}_R^{(\alpha)}\cdot\mathbf{E}_\infty \quad , \tag{4.21}$$

where $\mathbf{I}_T^{(\alpha)}$ and $\mathbf{I}_R^{(\alpha)}$ respectively denote interaction tensors between the particule $\mathcal{P}_\alpha$ and the other one. Indeed, the corrections to Smoluchowski's results are given by (4.21) and

$$\mathbf{U}^{(\alpha)} - \frac{\epsilon\zeta_\alpha}{\mu}\mathbf{E}_\infty = \frac{(-1)^\alpha\epsilon}{\mu}(\zeta_1 - \zeta_2)\mathbf{I}_T^{(\alpha)}\cdot\mathbf{E}_\infty \quad . \tag{4.22}$$

Above results (4.20), (4.22) hold for any two-particle cluster of uniformly charged particles (when embedded in a uniform electric field $\mathbf{E}_\infty$). Such behaviors (interaction terms linear in the difference $\zeta_1 - \zeta_2$) have been established for two-sphere clusters only by Reed and Morrison (1976) for two equal-size spheres and Keh and Chen (1989a, b) for arbitrary spheres. For two spheres $\mathcal{P}_1$ and $\mathcal{P}_2$ respectively of radius r_1 and r_2 and such that $d = x_3(1) - x_3(2) > r_1 + r_2$, those authors found that $\mathbf{I}_R^{(\alpha)}\cdot\mathbf{e}_3 = \mathbf{0}.\ \mathbf{e}_k\cdot\mathbf{I}_T^{(\alpha)}\cdot\mathbf{e}_3 = 0.\ \mathbf{e}_i\cdot\mathbf{I}_T^{(\alpha)}\cdot\mathbf{e}_k = 0$ if $i \neq k$ for $i \in \{1.2.3\}$ and $k \in \{1.2\}$ and calculated the following interaction coefficients

$$N_{12} = r_l\mathbf{e}_2\cdot\mathbf{I}_R^{(1)}.\mathbf{e}_1, \quad M_{12} = \mathbf{e}_1\cdot\mathbf{I}_T^{(1)}\cdot\mathbf{e}_1 = \mathbf{e}_2\cdot\mathbf{I}_T^{(1)}\cdot\mathbf{e}_2 \quad , \tag{4.23}$$

$$M'_{12} = \mathbf{e}_3\cdot\mathbf{I}_T^{(1)}\cdot\mathbf{e}_3, \quad M'_{21} = \mathbf{e}_3\cdot\mathbf{I}_T^{(2)}\cdot\mathbf{e}_3 \tag{4.24}$$

Table 2. Computed mobilities $\nu_i^{(\alpha)}$ for our ellipsoids with $a_1 = 1.2$, $b_1 = 10.8$, $c_1 = 1.0$, $a_2 = 0.8$, $b_2 = 1.0$, $c_2 = 1.2$ and $x_3(2) = 0$, $d = x_3(1) > 2.2$

d	$N_d(1) = N_d(2)$	$\max\lvert\nu_i^{(\alpha)}\rvert$ for (i_m, α_m)	(i_m, α_m)
2.3	242 = [6,1]	7.21E − 3	(2, 2)
2.3	434 = [10,1]	1.48E − 3	(2, 2)
2.4	74 = [4,0]	1.06E − 2	(2, 2)
2.4	242 = [6,1]	2.22E − 3	(2, 2)
2.4	434 = [10,1]	3.00E − 4	(2, 2)
5	74 = [4,0]	1.55E − 3	(1, 3)
5	242 = [6,1]	4.68E − 4	(1, 3)
5	434 = [10,1]	2.88E − 4	(1, 3)
10	74 = [4,0]	1.55E − 3	(1, 3)
10	242 = [6,1]	4.68E − 4	(1, 3)
10	434 = [10,1]	2.88E − 4	(1, 3)
30	242 = [6,1]	4.80E − 4	(1, 3)
100	242 = [6,1]	4.80E − 4	(1, 3)

for different ratio r_2/r_1 and dimensionless separation parameter

$$\lambda = \frac{r_1 + r_2}{d} \quad . \tag{4.25}$$

In evaluating N_{12}, M_{12} and M'_{12} we select $\zeta_1 = 0$ and $\zeta_2 = 1$ whilst M'_{21} is obtained by choosing $\zeta_1 = 1$ and $\zeta_2 = 0$.

Each computed coefficient is compared to its exact value (see Keh and Chen 1989a, b). As suggested by our previous comparisons for $\zeta_1 = \zeta_2$, we start with 74-node surface meshes. For $r_2/r_1 \in \{0.5, 1, 2\}$ this choice yields fine results (of 0.1% and 0.01% accuracy for (M'_{12}, M_{21}) and (M_{12}, N_{12}) respectively; see Tables 3 and 4) in the range $\lambda \geq 0.8$. However, as the gap thickness between spheres approaches zero (for $\lambda \to 1$) our meshes become too coarse and this results in discrepancies, especially for $r_2/r_1 = 5$. As shown in Table 5, mesh refinement makes it possible to remedy, if needed, to this loss of accuracy.

For symmetry reasons, if $r_2/r_1 = 1$ then $M'_{12} = M'_{21}$ and $N_{21} := r_2\mathbf{I}_R^{(2)}\cdot\mathbf{e}_1 = -N_{12}$. $M_{21} = \mathbf{I}_T^{(2)}\cdot\mathbf{e}_1 = M_{12}$. However, our numerical treatment differs for our identical spheres, at least because of the LU factorization algorithm and this yields non-zero computed quantities $M'_{12} - M'_{21}$. $N_{12} + N_{21}$ and $M_{12} - M_{21}$. As indicated in Table 3 for the difference $M'_{12} - M'_{21}$, our numerical scheme was actually found to preserve the required symmetry properties up to five digits even using 74 collocation points on each sphere. For example, one actually obtains $M'_{12} = 0.1055108$ and $M'_{21} = 0.1055078$ if $\lambda = 0.8$. Note that for $r_1 = r_2 = 1$ the functions $M'_{12} = M'_{21}$ is plotted versus λ in Fig. 3.

4.3
Numerical results for ellipsoids

The present method makes it possible to deal with particles of arbitrary shapes and potentials. For example, it is worth examining the dependence versus the center-to-center distance $d = O_1O_2$ of our interaction tensors $\mathbf{I}_T^{(\alpha)}$ and $\mathbf{I}_R^{(\alpha)}$ for two uniformly charged ellipsoids embedded in a uniform electric field $\mathbf{E}_\infty$. First, we consider two ellipsoids $\mathcal{P}_1$ and $\mathcal{P}_2$ such that (remind (4.9))

Table 3. Computed interaction coefficients M'_{12} and M'_{21} for two spheres and $N_d(1) = N_d(2) = 74 = [4,0]$

$\frac{r_2}{r_1}$	λ	Computed values		Exact values	
		M'_{12}	M'_{21}	M'_{12}	M'_{21}
	0.2	0.00101	0.00101	0.00101	0.00101
	0.6	0.03268	0.03268	0.03288	0.03288
$\frac{1.0}{1.0}$	0.8	0.10551	0.10551	0.10855	0.10855
	0.9	0.19749	0.19749	0.20969	0.20969
	0.2	0.00238	0.00030	0.00238	0.00030
	0.6	0.06859	0.01102	0.06975	0.01111
$\frac{2.0}{1.0}$	0.8	0.19291	0.03655	0.20588	0.03729
	0.9	0.33907	0.06893	0.37465	0.06985
	0.2	0.00465	0.00004	0.00463	0.00004
	0.6	0.12060	0.00157	0.12708	0.00159
$\frac{2.0}{0.4}$	0.8	0.27417	0.00481	0.32237	0.00486
	0.9	0.43166	0.00802	0.51300	0.00783

Table 4. Computed interaction coefficients M_{12} and N_{12} for two spheres and $N_d(1) = N_d(2) = 74 = [4,0]$

$\frac{r_2}{r_1}$	λ	Computed values		Exact values	
		$-M_{12}$	N_{12}	$-M_{12}$	N_{12}
	0.2	0.00015	1.06E-6	0.00015	3.56E-7
	0.6	0.00439	0.00085	0.00402	0.00087
$\frac{1.0}{2.0}$	0.8	0.01313	0.00689	0.01319	0.00714
	0.9	0.02381	0.01728	0.02435	0.01829
	0.2	0.00050	9.12E-7	0.00050	3.87E-7
	0.6	0.01406	0.00106	0.01395	0.00109
$\frac{1.0}{1.0}$	0.8	0.03745	0.00944	0.03747	0.01063
	0.9	0.06339	0.02613	0.06536	0.03274
	0.2	0.00119	1.06E-6	0.00119	1.75E-7
	0.6	0.03284	0.00046	0.03229	0.00065
$\frac{2.0}{1.0}$	0.8	0.08247	0.00414	0.08079	0.00878
	0.9	0.13011	0.01488	0.13066	0.03572

$$a_1 = 1.2, \quad b_1 = 0.8, \quad c_1 = 1.0, \quad x_3(1) = d > 2.2 \ , \tag{4.26}$$

$$a_2 = 0.8, \quad b_2 = 1.0, \quad c_2 = 1.2, \quad x_3(2) = 0 \ . \tag{4.27}$$

This configuration readily admits (O, x_1, x_3) and also (O, x_2, x_3) as planes of symmetry. Accordingly, many interaction coefficients $\mathbf{e}_i \cdot \mathbf{I}_L^{(\alpha)} \cdot \mathbf{e}_j$ vanish, for $L \in \{T, R\}$. The non-zero terms

$$T_{33}^{(\alpha)} = \mathbf{e}_3 \cdot \mathbf{I}_T^{(\alpha)} \cdot \mathbf{e}_3, \quad T_{kk}^{(\alpha)} = \mathbf{e}_k \cdot \mathbf{I}_T^{(\alpha)} \cdot \mathbf{e}_k \ , \tag{4.28}$$

$$R_{mk}^{(\alpha)} = \mathbf{e}_m \cdot \mathbf{I}_R^{(\alpha)} \cdot \mathbf{e}_k \tag{4.29}$$

for $m \in \{1,2\}$ and $k \in \{1,2\}$, only depend on the dimensionless separation parameter

$$\lambda = \frac{c_1 + c_2}{d} \ . \tag{4.30}$$

As suggested by the previous Sect. 2, we use only 74 collocation points on each ellipsoid and compute our non-zero quantities $\mathbf{e}_i \cdot \mathbf{I}_L^{(\alpha)} \cdot \mathbf{e}_j$ by selecting $(\zeta_1, \zeta_2) = (0,1)$ or $(\zeta_1, \zeta_2) = (1,0)$ respectively for $\alpha = 1$ or $\alpha = 2$. Computed results are plotted, versus λ, in Figs. 3–5. Each interaction coefficient is seen to dramatically increase in magnitude as the surface-to-surface spacing gets close to zero ($\lambda \to 1$) but is still large relative to the Debye length κ^{-1}. These behaviors result in strong interactions for close enough ellipsoids. Contrary to the case of two identical spheres (see Fig. 3) interaction coefficients $I_{33}^{(1)}$ and $I_{33}^{(2)}$ (slightly) differ. For particles more different in size, one expects larger differences $|I_{33}^{(1)} - I_{33}^{(2)}|$.

Table 5. Effects of mesh refinement for two near-touching spheres with $N_{dc} = N_d(1) = N_d(2)$ and $r_2/r_1 = 2.0/0.4$

N_{dc}	λ	M'_{12}	M'_{21}
242 = [6,1]	0.8	0.31567	0.00484
530 = [12,1]	0.8	0.32275	0.00486
Exact	0.8	0.32237	0.00486
242 = [6,1]	0.9	0.43166	0.00802
530 = [12,1]	0.9	0.51258	0.00782
Exact	0.9	0.51300	0.00783

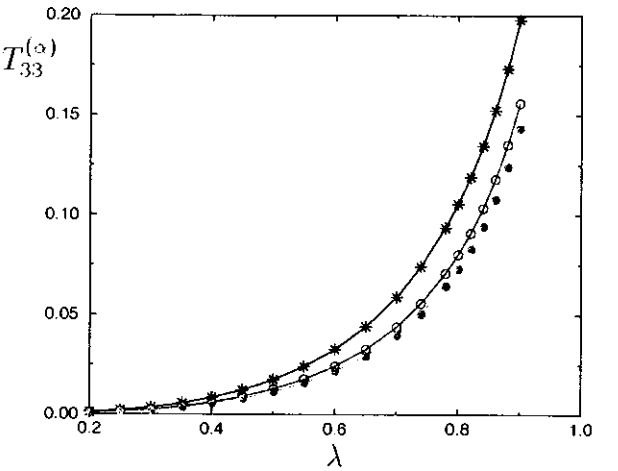

Fig. 3. Interactions coefficients $T_{33}^{(\alpha)}$ (see definition (4.28)) versus the separation variable λ. Coefficient $M'_{12} = M'_{21}$ for equal-size spheres with $r_1 = r_2$: (*). Coefficient $T_{33}^{(1)}$: (○) and coefficient $T_{33}^{(2)}$: (●)

For two spheres of unit radii, one obtains $N_{12} = R_{12}^{(1)} = R_{21}^{(2)} = -R_{12}^{(2)} = -R_{21}^{(1)} = -N_{21}$. As shown in Fig. 5, this is not at all the case for our ellipsoids (the coefficient $R_{21}^{(2)}$ is weak in the whole investigated domain $\lambda \leq 0.9$).

Of course, the strong dependence of the interaction coefficients upon the center-to-center distance d induces large variations of the electrophoretic mobilities $u_i^{(\alpha)}$ and $v_i^{(\alpha)}$ (see Def. (4.18)). For example, if we choose $\zeta_1 = 1$ and $\zeta_2 = \eta$, mobilities $u_3^{(1)}$ and $u_3^{(2)}$ are plotted versus d in Figs. 6 and 7 respectively for different values of η. Those electrophorectic mobilities clearly deeply depend on d for close ellipsoids.The first ellipsoid $\mathcal{P}_1$ (see Fig. 6) is speeded up or slowed down (with respect to the Smoluchowski solution) by the motion of the second one as soon as $\eta > 1$ or $\eta < 1$ respectively. For η negative and near contact particles (see, in Fig. 6, the curve pertaining to the case $\eta = -5$), the first ellipsoid may even experience a zero or negative mobility, i.e. change its direction of motion! On the contrary (see Fig. 7), the ellipsoid $\mathcal{P}_2$ is slowed down by $\mathcal{P}_1$ whatever η and d.

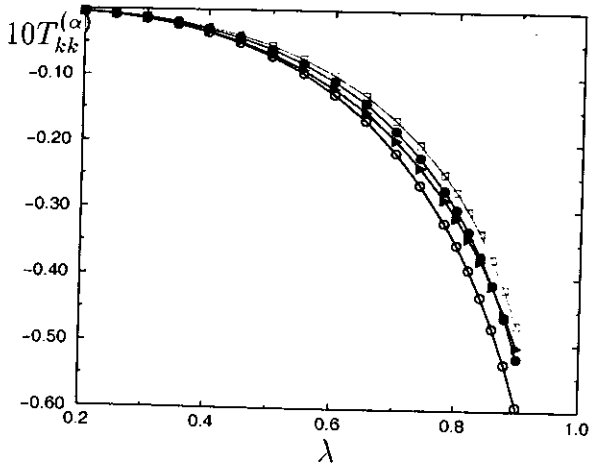

Fig. 4. Interactions coefficients $T_{kk}^{(\alpha)}$, for $k \in \{1,2\}$, versus the separation variable λ. Product $10T_{22}^{(1)}$: (○), product $10T_{22}^{(2)}$: (●), product $10T_{11}^{(1)}$: (□) and product $10T_{11}^{(2)}$: (▶)

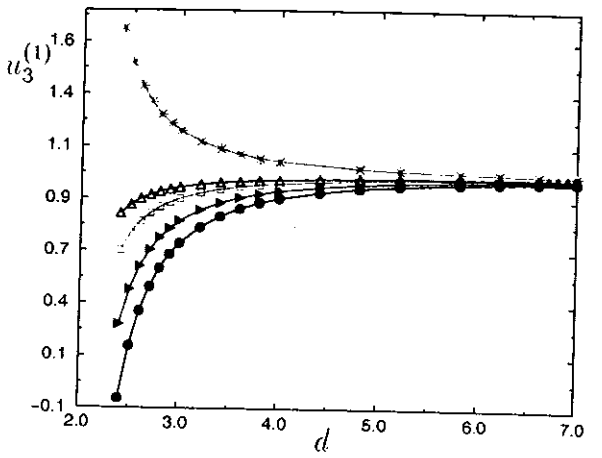

Fig. 6. Normalized electrophoretic mobility $u_3^{(1)}$ versus the center-to-center distance d for $\zeta_1 = 1$ and $\zeta_2 = \eta \cdot (*)$: $\eta = 5$, (○): $\eta = 3$, (Δ): $\eta = 0$, (□): $\eta = -1$, (▶): $\eta = -3$ and (●): $\eta = -5$

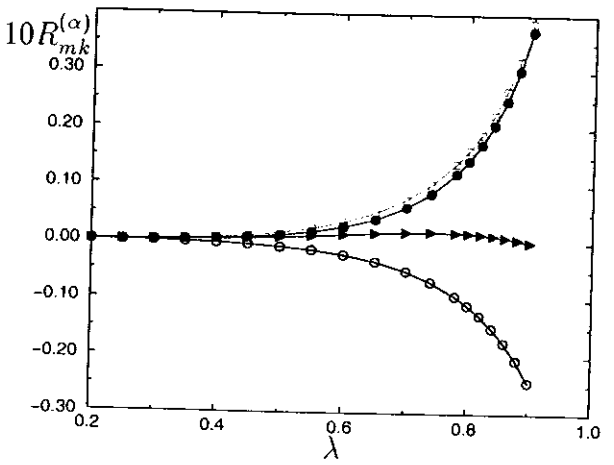

Fig. 5. Interactions coefficients $R_{mk}^{(\alpha)}$, for $k \neq m$, versus the separation variable λ. Product $10R_{12}^{(1)}$: (○), product $10R_{12}^{(2)}$: (●), product $10R_{21}^{(1)}$: (□) and product $10R_{21}^{(2)}$: (▶)

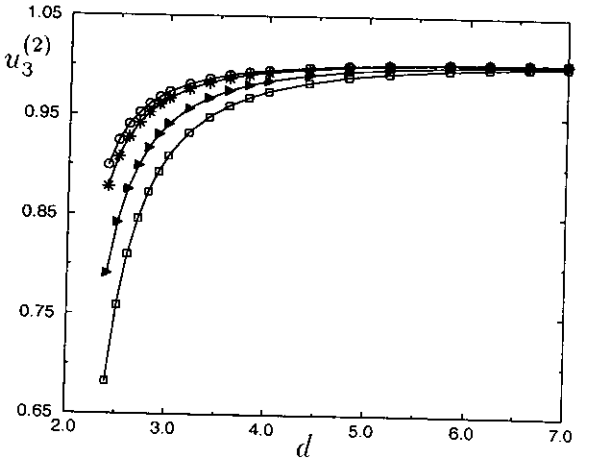

Fig. 7. Normalized electrophoretic mobility $u_3^{(2)}$ versus the center-to-center distance d for $\zeta_1 = 1$ and $\zeta_2 = \eta \cdot (*)$: $\eta = 5$, (○): $\eta = 3$, (□): $\eta = -1$ and (▶): $\eta = -3$

Finally we consider the case of identical spheroids. Two configurations are addressed:

(i) First configuration. Here we choose $a_1 = a_2 = b_1 = b_2 = 1.0, c_1 = c_2 = 2.0$ and $d = x_3(1) - x_3(2) > 4.0$. Again, for symmetry reasons the only non-zero interaction terms are still given by (4.28)–(4.29) and we set

$$T_{33} := T_{33}^{(1)} = T_{33}^{(2)} \ . \tag{4.31}$$

$$T_{22} := T_{22}^{(1)} = T_{22}^{(2)} = T_{11}^{(1)} = T_{11}^{(2)} \ . \tag{4.32}$$

(ii) Second configuration. This time $a_1 = a_2 = 2.0, b_1 = b_2 = c_1 = c_2 = 1.0$ and $d = x_3(1) - x_3(2) > 2.0$. In this case we look at the following non-zero coefficients

$$T'_{33} := T_{33}^{(1)} = T_{33}^{(2)} \ . \tag{4.33}$$

$$T'_{11} := T_{11}^{(1)} = T_{11}^{(2)}, \quad T'_{22} := T_{22}^{(1)} = T_{22}^{(2)} \ . \tag{4.34}$$

A 170-node mesh is used for each spheroid ($N_d(1) = N_d(2) = [8, 0]$) and the dependence of the computed coefficients upon the separation variable $\lambda = (c_1 + c_2)/d$ is illustrated in Figs. 8 and 9.

As revealed by Fig. 8 and 9, the behavior of one spheroid deeply depends upon the selected configuration: the differences $T_{33} - T'_{33}$ and $T_{22} - T'_{22}$ become large as the center-to-center distance d decreases.

5 Concluding remarks

Usually, one determines the electrophoretic motion of a two-particle cluster by calculating the perturbation electric potential and the electrolyte flow in the whole fluid domain. Such a task seems possible only for spheres and actually becomes a great numerical challenge in case of arbitrary configurations and shapes of the particles. The approach proposed in the present paper is free from these drawbacks and permits us to compute, at a reasonable cost, the rigid-body motion of any particle which may be of non-uniform zeta potential and embedded in a uniform or non-uniform electric field $\mathbf{E}_\infty$. Our method rests on the establishment and the numerical treatment of thirteen

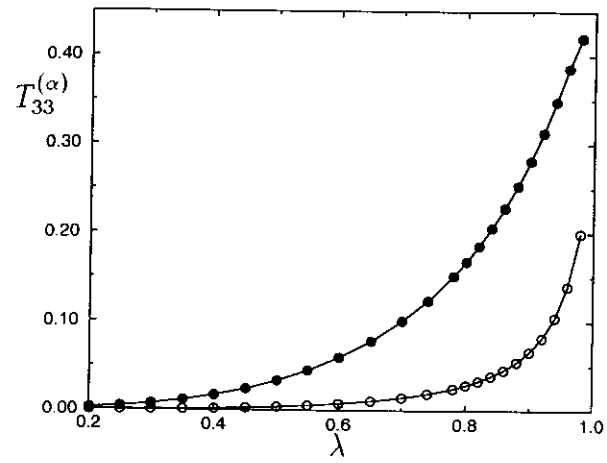

Fig. 8. Interactions coefficients $T_{33}^{(\alpha)}$, versus the separation variable λ, for two identical spheroids. Coefficient T_{33}: (○) and coefficient T'_{33}: (●)

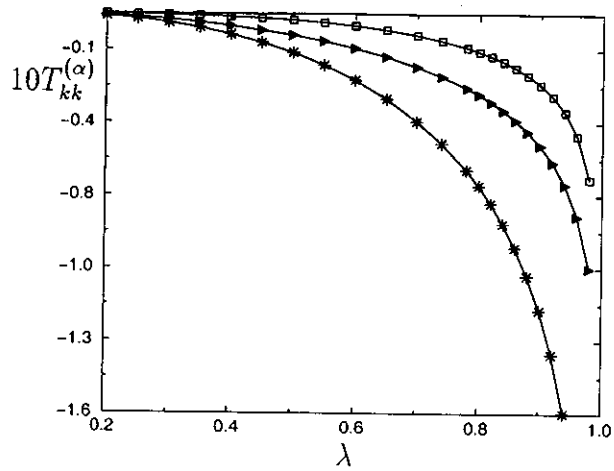

Fig. 9. Interactions coefficients $T_{kk}^{(\alpha)}$, versus the separation variable λ, for two identical spheroids. Product $10T_{22}$: (□), product $10T'_{11}$: (▶) and product $10T'_{22}$: (*)

boundary integral equations. The proposed numerical results perfectly agree with available analytical results for two-sphere clusters. For uniformly charged ellipsoids the interaction coefficients are found to deeply depend on the selected configuration.

In applications of electrophoresis, one usually encounters clusters of more than two particles. The advocated method is likely to apply to such circumstances. Such a task, which makes use of iterative methods and multipole approximations, is in current investigation.

References

1. **Acrivos A, Jeffrey DJ, Saville DA** (1990) Particle migration in suspensions by thermocapillary or electrophoretic motion. J. Fluid Mech. 212: 95–110
2. **Anderson JL** (1981) Concentration dependence of electrophoretic mobility. J. Colloid Interface Sci. 82: 248–250
3. **Anderson JL** (1989) Colloid transport by interfacial forces. Ann. Rev. Fluid Mech. 21: 61–99
4. **Beskos DE** (1987) Introduction to Boundary Element Methods. In: Beskos DE (ed), Computational Methods in Mechanics, Elsevier Science Publishers B. V., pp. 23–106
5. **Bonnet M** (1999) Boundary Integral Equation Methods for Solids and Fluids. John Wiley & Sons Ltd, New York
6. **Brebbia CA, Telles JCL, Wrobel LC** (1984) Boundary Element Techniques. Theory and Applications in Engineering, Springer-Verlag Berlin
7. **Chen B, Keh HJ** (1988) electrophoresis in a dilute dispersion of colloidal spheres. AIChE J. 34(7): 1075–1085
8. **Chen B, Keh HJ** (1989a) Particles interactions in electrophoresis: I. Motion of two spheres along their line of centers. J. Colloid Interface Sci. 130(2): 542–555
9. **Chen B, Keh HJ** (1989b) Particles interactions in electrophoresis: II. Motion of two spheres normal to their line of centers. J. Colloid Interface Sci. 130(2): 556–567
10. **Dautray R, Lions JL** (1988) Analyse mathématique et calcul numérique pour les sciences et les techniques. Vol 6, pp. 998–1010
11. **Happel J, Brenner H** (1973) Low Reynolds Number Hydrodynamics. Martinus Nijhoff, Leidon
12. **Hunter RJ** (1981) Zeta Potential in Colloid Science. Academic Press, New York
13. **Hiemenz PC, Rajagopalan R** (1986) Principles of Colloid and Surface Chemistry. Marcel Dekker, New York
14. **Kim S, Karrila SJ** (1991) Microhydrodynamics: Principles and Selected Applications. Butterworth, Boston
15. **Ladyzhenskaya OA** (1969) The Mathematical Theory of Viscous Incompressible Flow. Gordon & Breach, New York
16. **Lyness JN, Jespersen D** (1975) Moderate degree symmetric quadrature rules for the triangle. J. Inst. Math. Appl. 15: 19–32
17. **Morrison FA** (1970) Electrophoresis of a particle of arbitrary shape. J. Colloid Interface Sci. 34: 210–214
18. **Pozrikidis C** (1992) Boundary Integral and Singularity Methods for Linearized Viscous Flow. Cambridge University Press, Cambridge, UK
19. **Reed LD, Morrison FA** (1976) Hydrodynamic interactions in electrophoresis. J. Colloid Interface Sci. 54: 117–133
20. **Rezayat M, Shippy DJ, Rizzo FJ** (1986) On time-harmonic elastic-wave analysis by the boundary element method for moderate to high frequencies. Comp. Meth. Appl. Mech. Eng. 55: 349–367
21. **Sellier A** (2001) Electrophoresis of particles of equal and uniform zeta potentials in an unbounded electrolyte, in preparation
22. **Smoluchowski MV** (1921) In: Handbuch der Electrizitat und des Magnetismus. (ed) Graetz L Leipzig J. A. Barth, Chapter II pages 366–428
23. **Teubner M** (1982) The motion of charged colloidal particles in electric fields. J. Chem. Phys. 76(11): 5564–5573
24. **Trang-Cong T, Phan-Thien N** (1989) Stokes problems of multiparticle systems: a numerical method for arbitrary flows. Phys. Fluids A 1(3): 453–461